
Learning the Mechanism of Catastrophic Forgetting: A Perspective from Gradient Similarity

**Mutian Yang^{1*} Zisen Zhan^{2*} Yutong Chen¹ Haolin Li¹ Kaiwen Wang¹
Kaili Zheng¹ Yuguang Wang² Qi Wang^{3†} Jiandong Gao^{1†} Ji Wu^{1,4,5†}**

¹Department of Electronic Engineering, Tsinghua University, Beijing, China

²Institute of Medical Technology, Peking University Health Science Center, Peking University, Beijing, China

³College of Information Science and Engineering, Northeastern University, Shenyang, China

⁴College of AI, Tsinghua University, Beijing, China

⁵Beijing National Research Center for Information Science and Technology, Beijing, China

yangmutian@mail.tsinghua.edu.cn zisen_zhan_25@stu.pku.edu.cn
wangqi@ise.neu.edu.cn jdiao@tsinghua.edu.cn wuji_ee@tsinghua.edu.cn

Abstract

Catastrophic forgetting during knowledge injection severely undermines the continual learning capability of large language models (LLMs). While existing methods attempt to mitigate this issue, they often lack a foundational theoretical explanation. In this paper, we establish a theoretical framework from the perspective of gradient to explain catastrophic forgetting. First, we theoretically prove that strongly negative gradient similarity is the fundamental cause of catastrophic forgetting. Subsequently, gradient similarity is employed to identify two types of neurons during catastrophic forgetting: conflicting neurons, which induce forgetting and account for 50%–75% of all neurons, and collaborative neurons, which mitigate forgetting and account for 25%–50%. Ultimately, a novel knowledge injection method named **Collaborative Neural Learning (CNL)** is proposed. By freezing conflicting neurons and only updating collaborative neurons, CNL theoretically eliminates catastrophic forgetting under the assumption of an infinitesimal learning rate η and exactly known Mastered Set. Studies on five LLMs, four datasets, and four optimizers prove that CNL achieves zero forgetting under in-set experiments, and reduces the level of catastrophic forgetting by 59.1%–81.7% under out-of-set experiments.

1 Introduction

Large language models (LLMs) have shown exceptional knowledge capacity and achieved remarkable potential across a broad range of domains Achiam et al. (2023); Touvron et al. (2023). To continuously expand their knowledge breadth, various knowledge injection methods have been proposed Lewis et al. (2020); Wang et al. (2024); Ke et al. (2023). Although these methods enable LLMs to acquire new knowledge, they also cause the forgetting of previously mastered knowledge Zhou et al. (2025). This phenomenon, known as catastrophic forgetting Korbak et al. (2022), severely hinders the continual improvement of LLMs Zhou et al. (2024). To mitigate catastrophic forgetting, it is crucial to understand its underlying mechanisms.

^{*}Equal Contribution

[†]Corresponding Author

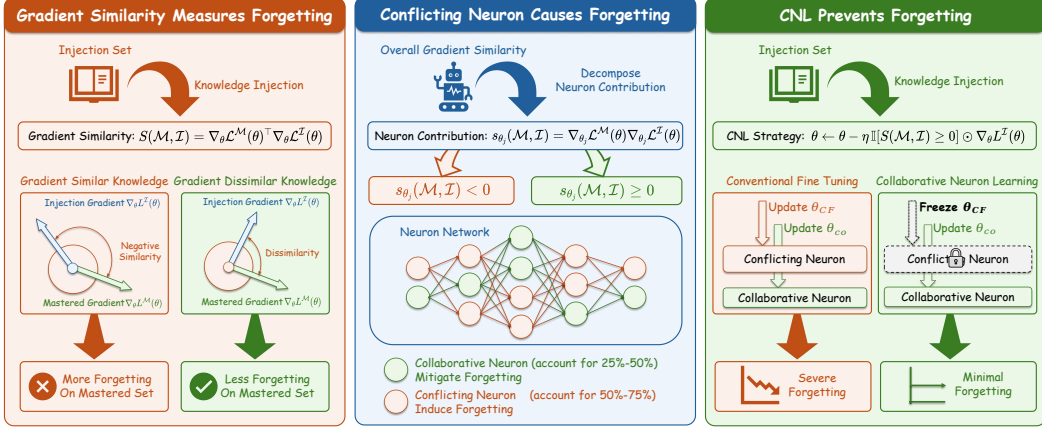


Figure 1: Conceptual illustration of our framework. We reveal the mechanism of catastrophic forgetting and propose a novel method to prevent its occurrence from a perspective of gradient similarity.

Recent studies have attempted to analyze catastrophic forgetting from a “similarity” perspective Bai et al. (2024); Wu et al. (2024). Specifically, they measure the similarity between injected knowledge and previously mastered knowledge using embedding representations Mitchell et al. (2022) and knowledge graphs Tan et al. (2025); Zhu et al. (2025). Results show that knowledge highly similar to injected knowledge is more likely to be forgotten Luo et al. (2025); Li et al. (2024). While these studies provide valuable insights into catastrophic forgetting, they fail to rigorously and theoretically reveal its underlying mechanisms.

Additionally, numerous approaches have been proposed to mitigate catastrophic forgetting, including replay based Huang et al. (2024), parameter-efficient fine-tuning based Li et al. (2025), and knowledge editing based approaches Ge et al. (2024). While they alleviate forgetting to some extent, they lack a rigorous theoretical foundation and therefore cannot avoid catastrophic forgetting at theoretically.

Our work explores the mechanisms of catastrophic forgetting through both theoretical analysis and experimental validation. More specifically, we seek to answer the following three key questions regarding catastrophic forgetting:

- What conditions lead to catastrophic forgetting? In Section 3, we demonstrate through rigorous theoretical derivation and extensive empirical results that strongly negative gradient similarity between injected knowledge and mastered knowledge underlies catastrophic forgetting.
- Which neurons are responsible for catastrophic forgetting? In Section 4, we apply gradient similarity to reveal two distinct types of neurons: conflicting neurons and collaborative neurons. Conflicting neurons induce forgetting and comprise 50%–75% of all neurons, whereas collaborative neurons alleviate forgetting and constitute 25%–50%.
- How to prevent catastrophic forgetting? In Section 5, we propose a novel knowledge injection method, CNL, which freezes conflicting neurons and trains collaborative neurons. CNL theoretically prevent forgetting under the assumption of an infinitesimal learning rate η and exactly known Mastered Set. Experiments on five models, four datasets, and four optimizers demonstrate CNL effectively mitigates forgetting under both in-set and out-of-set conditions.

To ensure the reproducibility of this study, all of the codes and datasets are included in Supplementary Material. Code and datasets are available at: <https://github.com/yangmutian/Collaborative-Neuron-Learning>

2 Definition of Learning and Forgetting from the Perspective of Gradient

2.1 Learning

The neural network of LLMs is defined as $f_{\theta} : \mathcal{X} \rightarrow \mathcal{Y}$, where the mapping from the input space to the output space is determined by parameters $\theta = (\theta_1, \dots, \theta_{|\theta|}) \in \mathbb{R}^{|\theta|}$.

Let \mathcal{I} denote a set of knowledge samples to be injected

$$\mathcal{I} = \{(x_1^{\mathcal{I}}, y_1^{\mathcal{I}}), \dots, (x_{|\mathcal{I}|}^{\mathcal{I}}, y_{|\mathcal{I}|}^{\mathcal{I}})\} \quad (1)$$

Loss on a single injection sample $(x, y) \in \mathcal{I}$ is expressed as $L^{(x,y)}(\theta) = \ell(f_{\theta}(x), y)$, where $\ell(\cdot, \cdot)$ denotes the loss function. The total loss on Injection Set \mathcal{I} is expressed as the mean loss over all samples

$$\begin{aligned} \mathcal{L}^{\mathcal{I}}(\theta) &= \frac{1}{|\mathcal{I}|} \sum_{(x,y) \in \mathcal{I}} L^{(x,y)}(\theta) \\ &= \frac{1}{|\mathcal{I}|} \sum_{(x,y) \in \mathcal{I}} \ell(f_{\theta}(x), y) \end{aligned} \quad (2)$$

Let $\nabla_{\theta} \mathcal{L}^{\mathcal{I}}(\theta) \in \mathbb{R}^{|\theta| \times 1}$ denote the gradient of $\mathcal{L}^{\mathcal{I}}(\theta)$ with respect to θ . Under gradient descent with a learning rate η , the parameter update is given by

$$\theta \leftarrow \theta - \eta \nabla_{\theta} \mathcal{L}^{\mathcal{I}}(\theta) \quad (3)$$

Assuming an infinitesimal learning rate η , the loss after parameter update can be approximated using a first-order Taylor expansion

$$\begin{aligned} &\mathcal{L}^{\mathcal{I}}(\theta - \eta \nabla_{\theta} \mathcal{L}^{\mathcal{I}}(\theta)) \\ &= \frac{1}{|\mathcal{I}|} \sum_{(x,y) \in \mathcal{I}} [L^{(x,y)}(\theta - \eta \nabla_{\theta} \mathcal{L}^{\mathcal{I}}(\theta))] \\ &\approx \frac{1}{|\mathcal{I}|} \sum_{(x,y) \in \mathcal{I}} \left[L^{(x,y)}(\theta) - \eta \nabla_{\theta} L^{(x,y)}(\theta)^{\top} \nabla_{\theta} \mathcal{L}^{\mathcal{I}}(\theta) \right] \\ &= \mathcal{L}^{\mathcal{I}}(\theta) - \eta \nabla_{\theta} \mathcal{L}^{\mathcal{I}}(\theta)^{\top} \nabla_{\theta} \mathcal{L}^{\mathcal{I}}(\theta) \end{aligned} \quad (4)$$

Therefore, the change in loss is:

$$\begin{aligned} \Delta \mathcal{L}^{\mathcal{I}} &= \mathcal{L}^{\mathcal{I}}(\theta - \eta \nabla_{\theta} \mathcal{L}^{\mathcal{I}}(\theta)) - \mathcal{L}^{\mathcal{I}}(\theta) \\ &= -\eta \nabla_{\theta} \mathcal{L}^{\mathcal{I}}(\theta)^{\top} \nabla_{\theta} \mathcal{L}^{\mathcal{I}}(\theta) \end{aligned} \quad (5)$$

Since $\nabla_{\theta} \mathcal{L}^{\mathcal{I}}(\theta)$ is column vector, $\nabla_{\theta} \mathcal{L}^{\mathcal{I}}(\theta)^{\top} \nabla_{\theta} \mathcal{L}^{\mathcal{I}}(\theta)$ represents the inner product of the gradient with itself. We define the **Gradient Similarity** as

$$S(\mathcal{I}, \mathcal{I}) = \nabla_{\theta} \mathcal{L}^{\mathcal{I}}(\theta)^{\top} \nabla_{\theta} \mathcal{L}^{\mathcal{I}}(\theta) \quad (6)$$

Due to the non-negativity of the inner product, we have $\Delta \mathcal{L}^{\mathcal{I}} = -\eta S(\mathcal{I}, \mathcal{I}) \leq 0$. In practice, parameter updates are rarely zero strictly, leading to

$$\Delta \mathcal{L}^{\mathcal{I}} = -\eta S(\mathcal{I}, \mathcal{I}) < 0 \quad (7)$$

This derivation defines the process of learning: under a sufficiently small learning rate η , knowledge injection monotonically decreases the loss on Injection Set \mathcal{I} .

2.2 Forgetting

Subsequently, we analyze the impact of knowledge injection on samples with mastered knowledge, denoted as Mastered Set

$$\mathcal{M} = \{(x_1^{\mathcal{M}}, y_1^{\mathcal{M}}), \dots, (x_{|\mathcal{M}|}^{\mathcal{M}}, y_{|\mathcal{M}|}^{\mathcal{M}})\} \quad (8)$$

The loss on Mastered Set is defined as $\mathcal{L}^{\mathcal{M}}(\theta)$. After parameter update according to Eq. (3), the loss becomes $\mathcal{L}^{\mathcal{M}}(\theta - \eta \nabla_{\theta} \mathcal{L}^{\mathcal{I}}(\theta))$. Assuming an infinitesimal learning rate η , the expression is expanded through first-order Taylor approximation:

$$\begin{aligned} &\mathcal{L}^{\mathcal{M}}(\theta - \eta \nabla_{\theta} \mathcal{L}^{\mathcal{I}}(\theta)) \\ &= \frac{1}{|\mathcal{M}|} \sum_{(x,y) \in \mathcal{M}} L^{(x,y)}(\theta - \eta \nabla_{\theta} \mathcal{L}^{\mathcal{I}}(\theta)) \\ &\approx \frac{1}{|\mathcal{M}|} \sum_{(x,y) \in \mathcal{M}} \left[L^{(x,y)}(\theta) - \eta \nabla_{\theta} L^{(x,y)}(\theta)^{\top} \nabla_{\theta} \mathcal{L}^{\mathcal{I}}(\theta) \right] \\ &= \mathcal{L}^{\mathcal{M}}(\theta) - \eta \nabla_{\theta} \mathcal{L}^{\mathcal{M}}(\theta)^{\top} \nabla_{\theta} \mathcal{L}^{\mathcal{I}}(\theta) \end{aligned} \quad (9)$$

The change in loss is expressed as

$$\begin{aligned}\Delta \mathcal{L}^{\mathcal{M}} &= \mathcal{L}^{\mathcal{M}}(\theta - \eta \nabla_{\theta} \mathcal{L}^{\mathcal{I}}(\theta)) - \mathcal{L}^{\mathcal{M}}(\theta) \\ &= -\eta \nabla_{\theta} \mathcal{L}^{\mathcal{M}}(\theta)^{\top} \nabla_{\theta} \mathcal{L}^{\mathcal{I}}(\theta)\end{aligned}\quad (10)$$

We define the Gradient Similarity between Mastered Set \mathcal{M} and Injection Set \mathcal{I} as

$$S(\mathcal{M}, \mathcal{I}) = \nabla_{\theta} \mathcal{L}^{\mathcal{M}}(\theta)^{\top} \nabla_{\theta} \mathcal{L}^{\mathcal{I}}(\theta) \quad (11)$$

Therefore, during knowledge injection, the loss change on Mastered Set is given by

$$\Delta \mathcal{L}^{\mathcal{M}} = -\eta S(\mathcal{M}, \mathcal{I}) \quad (12)$$

Eq. (12) reveals a critical insight: the loss on the Mastered Set increases when the gradient similarity is negative. Therefore, mastered samples with more negative gradient similarity (i.e., stronger alignment in the opposite direction) are more susceptible to catastrophic forgetting.

3 Gradient Similarity Measures Catastrophic Forgetting

To validate the conclusion of Eq. (12), experiments on five models and four datasets were conducted.

3.1 Experiment Procedure

Datasets: We employed standard benchmarks including Massive Multitask Language Understanding (MMLU) Hendrycks et al. (2020), Medical Question Answering (MedQA) Jin et al. (2021), AI2 Reasoning Challenge (ARC-C) Clark et al. (2018), and Commonsense Question Answering (CSQA) Talmor et al. (2019). The detailed information of datasets is shown in Appendix A.

Models: The experiments were conducted on *Qwen* Yang et al. (2024) and *LLaMA* Grattafiori et al. (2024) families, including *Qwen2.5 1.5B*, *Qwen2.5 3B*, *Qwen2.5 7B*, *LLaMA3.2 1B*, and *LLaMA3.2 3B*.

3.2 Catastrophic Forgetting Happens during Knowledge Injection

To distinguish Injection Set \mathcal{I} and Mastered Set \mathcal{M} , LLMs were asked to answer the questions in datasets (inference details in Appendix B). Correctly answered questions were categorized into \mathcal{M} , while incorrect ones formed \mathcal{I} . Appendix C exhibits the distribution of Injection Set \mathcal{I} and Mastered Set \mathcal{M} .

Subsequently, LLMs were trained on Injection Set \mathcal{I} for knowledge injection (training details in Appendix D). The correctly answered samples in Injection Set \mathcal{I} were used to evaluate learning, while the incorrectly answered samples in Mastered Set \mathcal{M} were used to measure forgetting. Results in Appendix E reveal that while LLMs successfully learn new knowledge from Injection Set \mathcal{I} , they simultaneously suffer forgetting on Mastered Set \mathcal{M} .

Notably, we extended our evaluation to parameter-efficient fine-tuning (PEFT) methods and observed that techniques like Low-Rank Adaptation (LoRA) Hu et al. (2022) could not mitigate this catastrophic forgetting. Detailed experimental settings and results are provided in Appendix F.

3.3 Strongly Negative Gradient Similarity Leads to Forgetting

Ultimately, gradient similarities between samples in Mastered Set \mathcal{M} and Injection Set \mathcal{I} were computed. In light of Eq. (12), samples with negative gradient similarity were ranked by the magnitude of their similarity. The top 1/3 with the largest magnitudes were assigned to the “Sim” group, representing strongly negative similarity, while the bottom 1/3 were assigned to the “Dissim” group.

Results in Table 1 indicate that catastrophic forgetting is predominantly concentrated in the “Sim” group. This empirical evidence provides strong support for Eq. (12), confirming that strongly negative gradient similarity drives catastrophic forgetting.

Table 1: Relationship between gradient similarity and catastrophic forgetting. Results are reported in the format of ‘‘Number of forgotten questions (Percentage)’’. Samples with negative gradient similarity were ranked by magnitude: the top 1/3 with the largest magnitudes were labeled ‘‘Sim’’ (High Negative Similarity), while the bottom 1/3 were labeled ‘‘Dissim’’. Results indicate that catastrophic forgetting occurs primarily in the ‘‘Sim’’ group.

MODEL	MMLU		MEDQA		ARC-C		CSQA	
	DISSIM	SIM	DISSIM	SIM	DISSIM	SIM	DISSIM	SIM
<i>Qwen 1.5B</i>	4 (1.4%)	137 (48.9%)	37 (20.6%)	113 (62.8%)	3 (1.0%)	72 (23.2%)	10 (3.7%)	102 (38.1%)
<i>Qwen 3B</i>	0 (0.0%)	118 (37.9%)	0 (0.0%)	113 (54.6%)	7 (2.0%)	193 (56.4%)	0 (0.0%)	84 (31.5%)
<i>Qwen 7B</i>	3 (0.9%)	120 (36.0%)	3 (1.2%)	116 (46.0%)	0 (0.0%)	17 (5.1%)	0 (0.0%)	40 (13.7%)
<i>LLaMA 1B</i>	0 (0.0%)	68 (58.6%)	0 (0.0%)	43 (42.2%)	6 (6.6%)	91 (100%)	9 (10.1%)	89 (100.0%)
<i>LLaMA 3B</i>	0 (0.0%)	83 (33.2%)	28 (11.1%)	32 (12.6%)	1 (0.4%)	73 (25.9%)	0 (0.0%)	34 (13.6%)

4 Conflicting Neurons Cause Catastrophic Forgetting

While LLMs exhibit overall forgetting on Mastered Set, it remains unclear whether forgetting is driven by all neurons or only a subset. Herein, gradient similarity is employed to identify the neurons contributing to forgetting. It should be clarified that in this paper, ‘‘neurons’’ and ‘‘parameters’’ carry essentially the same meaning. We use parameters when emphasizing their vector form for computation, and neurons when emphasizing their count.

The gradient similarity of the j -th neuron θ_j between Mastered Set \mathcal{M} and Injection Set \mathcal{I} is defined as

$$s_{\theta_j}(\mathcal{M}, \mathcal{I}) = \nabla_{\theta_j} \mathcal{L}^{\mathcal{M}}(\theta) \nabla_{\theta_j} \mathcal{L}^{\mathcal{I}}(\theta) \quad (13)$$

$\nabla_{\theta_j} \mathcal{L}^{\mathcal{M}}(\theta)$ and $\nabla_{\theta_j} \mathcal{L}^{\mathcal{I}}(\theta)$ represent the components of gradients on θ_j for Mastered and Injection Set, respectively.

The global gradient similarity of LLMs is equivalent to the sum of gradient similarities of individual neurons. Therefore, Eq. (11) is expressed as

$$\begin{aligned} S(\mathcal{M}, \mathcal{I}) &= \nabla_{\theta} \mathcal{L}^{\mathcal{M}}(\theta)^\top \nabla_{\theta} \mathcal{L}^{\mathcal{I}}(\theta) \\ &= \sum_{j=1}^{|\theta|} (\nabla_{\theta_j} \mathcal{L}^{\mathcal{M}}(\theta) \nabla_{\theta_j} \mathcal{L}^{\mathcal{I}}(\theta)) \\ &= \sum_{j=1}^{|\theta|} s_{\theta_j}(\mathcal{M}, \mathcal{I}) \end{aligned} \quad (14)$$

According to Eq. (12), if the gradient similarity of neuron θ_j with respect to Mastered Set \mathcal{M} and Injection Set \mathcal{I} is negative, this neuron contributes to an increase in loss and induce forgetting. We refer to such neurons as **Conflicting Neurons**. The set of conflicting neurons is defined as

$$\theta_{CF} := \{\theta_j \mid s_{\theta_j}(\mathcal{M}, \mathcal{I}) < 0\} \quad (15)$$

Conversely, if the gradient similarity of neuron θ_j is positive, this neuron contributes to a decrease in loss and mitigate forgetting. Such neurons are referred as **Collaborative Neurons**. The set of collaborative neurons is defined as

$$\theta_{CB} := \{\theta_j \mid s_{\theta_j}(\mathcal{M}, \mathcal{I}) \geq 0\} \quad (16)$$

Table 2 presents that nearly 25%-50% of neurons contribute to positive gradient similarity and are termed collaborative neurons, while 50%-75% of neurons contribute to negative gradient similarity and are termed conflicting neurons. These collaborative neurons are insufficient to counteract the effect of conflicting neurons, thereby leading to the phenomenon of catastrophic forgetting in LLMs.

Table 2: Distribution of collaborative neurons (COLL) and conflicting neurons (CONF). "PROP" represents the proportion of a specific neuron type relative to the total number of neurons. "GRAD" represents the gradient similarity sum for that neuron type. "TOTAL" represents the gradient similarity sum for all neurons. Typically, collaborative neurons account for 25%–50% of all neurons, while conflicting neurons account for 50%–75%.

MODEL	METRIC	MMLU		MEDQA		ARC-C		CSQA	
		COLL	CONF	COLL	CONF	COLL	CONF	COLL	CONF
<i>Qwen 1.5B</i>	PROP	47.7%	52.3%	42.1%	57.9%	49.7%	50.3%	48.4%	51.6%
	GRAD	+692	-1851	+567	-3186	+635	-1021	+577	-1438
	TOTAL	-1159		-2619		-386		-861	
<i>Qwen 3B</i>	PROP	49.4%	50.6%	44.6%	55.4%	51.7%	48.3%	52.9%	47.1%
	GRAD	+1626	-2979	+1538	-4319	+2237	-2569	+2703	-3276
	TOTAL	-1353		-2781		-332		-573	
<i>Qwen 7B</i>	PROP	49.6%	50.4%	49.0%	51.0%	51.2%	48.8%	51.6%	48.4%
	GRAD	+710	-1242	+661	-1282	+433	-664	+687	-940
	TOTAL	-532		-621		-231		-253	
<i>LLaMA 1B</i>	PROP	34.1%	65.9%	24.0%	76.0%	28.6%	71.4%	42.1%	57.9%
	GRAD	+2116	-64263	+54	-116388	+373	-88549	+4349	-41111
	TOTAL	-62147		-116334		-88176		-36762	
<i>LLaMA 3B</i>	PROP	37.8%	62.2%	30.4%	69.6%	46.5%	53.5%	42.7%	57.3%
	GRAD	+282	-2528	+116	-2784	+734	-2161	+404	-2178
	TOTAL	-2246		-2668		-1427		-1774	

This result reveals the coexistence of two types of neurons during catastrophic forgetting, which provide theoretical foundation for the following knowledge injection method.

5 Preventing Catastrophic Forgetting by Freezing Conflicting Neurons

Since conflicting neurons are responsible for catastrophic forgetting, a natural question arises: can catastrophic forgetting be avoided by freezing conflicting neurons and training only collaborative neurons? We refer to this learning paradigm as **Collaborative Neuron Learning** (CNL).

5.1 Establishment of CNL

To indicate the sign of gradient similarity for the j -th neuron, we define an indicator function $I(\cdot)$ as

$$I(s_{\theta_j}(\mathcal{M}, \mathcal{I}) \geq 0) = \begin{cases} 1, & \text{if } s_{\theta_j}(\mathcal{M}, \mathcal{I}) \geq 0 \\ 0, & \text{if } s_{\theta_j}(\mathcal{M}, \mathcal{I}) < 0 \end{cases} \quad (17)$$

Applying the indicator function to all neurons yields

$$\begin{aligned} & \mathbb{I}[S(\mathcal{M}, \mathcal{I}) \geq 0] \\ &= (I(s_{\theta_1}(\mathcal{M}, \mathcal{I}) \geq 0), \dots, I(s_{\theta_{|\theta|}}(\mathcal{M}, \mathcal{I}) \geq 0))^{\top} \end{aligned} \quad (18)$$

CNL freezes neurons with negative gradient similarity, leading to a parameter update rule defined as

$$\theta \leftarrow \theta - \eta \mathbb{I}[S(\mathcal{M}, \mathcal{I}) \geq 0] \odot \nabla_{\theta} L^{\mathcal{I}}(\theta) \quad (19)$$

where \odot denotes the Hadamard (element-wise) product. According to Eq. (9), the change in loss on Mastered Set \mathcal{M} after parameter update is given by

$$\begin{aligned} & \Delta L^{\mathcal{M}}(\theta) \\ &= -\eta \nabla_{\theta} L^{\mathcal{M}}(\theta)^{\top} (\mathbb{I}[S(\mathcal{M}, \mathcal{I}) \geq 0] \odot \nabla_{\theta} L^{\mathcal{I}}(\theta)) \\ &= -\eta \sum_{j=1}^{|\theta|} \left[\nabla_{\theta_j} L^{\mathcal{M}}(\theta) I(s_{\theta_j}(\mathcal{M}, \mathcal{I}) \geq 0) \nabla_{\theta_j} L^{\mathcal{I}}(\theta) \right] \\ &= -\eta \sum_{j=1}^{|\theta|} \left[I(s_{\theta_j}(\mathcal{M}, \mathcal{I}) \geq 0) s_{\theta_j}(\mathcal{M}, \mathcal{I}) \right] \end{aligned} \quad (20)$$

Table 3: Effectiveness of knowledge injection using FT and CNL. Results are reported in the format of ‘‘Number of questions (Percentage)’’. FT leads to the forgetting of previously mastered knowledge comparable in magnitude to the newly injected knowledge, whereas CNL induces negligible catastrophic forgetting.

MODEL	METHOD	MMLU		MEDQA		ARC-C		CSQA	
		LEARNED	FORGOT	LEARNED	FORGOT	LEARNED	FORGOT	LEARNED	FORGOT
<i>Qwen 1.5B</i>	FT	168 (24.8%)	188 (21.4%)	191 (27.1%)	264 (46.5%)	104 (32.1%)	88 (9.3%)	86 (31.6%)	163 (19.8%)
	CNL	168 (24.8%)	0 (0.0%)	193 (27.4%)	0 (0.0%)	163 (50.3%)	0 (0.0%)	147 (54.0%)	0 (0.0%)
<i>Qwen 3B</i>	FT	114 (19.5%)	126 (13.0%)	119 (18.6%)	160 (25.3%)	71 (33.5%)	286 (27.0%)	77 (31.7%)	105 (12.3%)
	CNL	116 (19.8%)	0 (0.0%)	119 (18.6%)	0 (0.0%)	76 (35.8%)	0 (0.0%)	81 (33.3%)	0 (0.0%)
<i>Qwen 7B</i>	FT	127 (28.0%)	193 (17.5%)	110 (21.9%)	169 (21.9%)	62 (46.3%)	19 (1.7%)	68 (34.5%)	48 (5.3%)
	CNL	189 (41.6%)	0 (0.0%)	249 (49.6%)	0 (0.0%)	90 (67.2%)	0 (0.0%)	144 (73.1%)	0 (0.0%)
<i>LLaMA 1B</i>	FT	158 (14.0%)	73 (17.0%)	105 (11.0%)	43 (13.4%)	328 (34.4%)	154 (48.7%)	333 (47.8%)	176 (44.1%)
	CNL	201 (17.9%)	0 (0.0%)	112 (11.8%)	0 (0.0%)	335 (35.1%)	0 (0.0%)	338 (48.5%)	0 (0.0%)
<i>LLaMA 3B</i>	FT	133 (18.3%)	96 (11.6%)	113 (22.2%)	101 (13.2%)	85 (24.5%)	76 (8.2%)	60 (19.5%)	35 (4.4%)
	CNL	133 (18.3%)	0 (0.0%)	125 (24.6%)	0 (0.0%)	86 (24.8%)	0 (0.0%)	63 (20.5%)	0 (0.0%)

In practical settings, it is almost impossible for all parameter gradients to be exactly zero. Therefore, we have

$$\begin{aligned} & \Delta L^{\mathcal{M}}(\theta) \\ &= -\eta \sum_{j=1}^{|\theta|} \left[I(s_{\theta_j}(\mathcal{M}, \mathcal{I}) \geq 0) s_{\theta_j}(\mathcal{M}, \mathcal{I}) \right] < 0 \end{aligned} \quad (21)$$

This result indicates that, under the assumption of an infinitesimally small learning rate η , CNL guarantees a monotonic decrease of the loss on Mastered Set \mathcal{M} . In other words, CNL theoretically prevents catastrophic forgetting.

To experimentally evaluate the effectiveness of CNL, we performed knowledge injection using both CNL and conventional fine tuning (FT). Their forgetting was compared under the constraint that CNL learned at least as many new samples as FT. As shown in Table 3, FT forgets a number of mastered samples comparable to the amount of newly injected knowledge, whereas CNL achieve zero forgetting.

Although CNL exhibits excellent performance in preventing forgetting, **we have to point out that CNL achieves zero forgetting only under two restrictive conditions:** (i) the learning rate η is sufficiently small, and (ii) Mastered Set \mathcal{M} is explicitly known. The case where Mastered Set \mathcal{M} is not explicitly available will be discussed in Section 5.4.

5.2 Extending CNL to More Complex Optimizers

After establishing CNL with Stochastic Gradient Descent (SGD) optimizer Rumelhart et al. (1985), we further extend CNL to Momentum Rumelhart et al. (1985), Adam Kingma (2014), AdamW Loshchilov and Hutter (2019), and arbitrary optimizer.

In Appendix G, rigorous proofs are provided that the loss on Mastered Set decreases monotonically, as long as the parameter update of Momentum, Adam, AdamW, arbitrary optimizer follows Eq. (27), (38), (43), and (58).

Table 4 demonstrates the experimental results of CNL with difference optimizers. When FT is applied, all four optimizers suffer from severe catastrophic forgetting. In contrast, CNL effectively prevents

Table 4: Comparison of knowledge injection performance across different optimizers. *Qwen2.5 1.5B* is selected for experiment. Whether using SGD, Momentum, Adam, or AdamW, CNL consistently achieves zero catastrophic forgetting while maintaining effective knowledge injection.

OPTIMIZER	METHOD	MMLU		MEDQA		ARC-C		CSQA	
		LEARNED	FORGOT	LEARNED	FORGOT	LEARNED	FORGOT	LEARNED	FORGOT
SGD	FT	168 (24.8%)	188 (21.4%)	191 (27.1%)	264 (46.5%)	104 (32.1%)	88 (9.3%)	86 (31.6%)	163 (19.8%)
	CNL	168 (24.8%)	0 (0.0%)	193 (27.1%)	0 (0.0%)	163 (50.3%)	0 (0.0%)	147 (54.0%)	0 (0.0%)
MOMENTUM	FT	341 (50.3%)	450 (51.3%)	257 (36.5%)	398 (70.1%)	261 (80.6%)	169 (17.9%)	205 (75.4%)	233 (28.3%)
	CNL	408 (60.2%)	0 (0.0%)	461 (65.5%)	0 (0.0%)	291 (89.8%)	0 (0.0%)	240 (88.2%)	0 (0.0%)
ADAM	FT	647 (95.4%)	203 (23.1%)	704 (100.0%)	181 (31.9%)	320 (98.8%)	143 (15.1%)	266 (97.8%)	168 (20.4%)
	CNL	648 (95.6%)	0 (0.0%)	704 (100.0%)	0 (0.0%)	323 (99.7%)	0 (0.0%)	266 (97.8%)	0 (0.0%)
ADAMW	FT	638 (94.1%)	195 (22.2%)	703 (99.9%)	174 (30.6%)	320 (98.8%)	143 (15.1%)	251 (92.3%)	294 (35.7%)
	CNL	642 (94.7%)	0 (0.0%)	703 (99.9%)	0 (0.0%)	323 (99.7%)	0 (0.0%)	266 (97.8%)	0 (0.0%)

catastrophic forgetting across all four optimizers. In particular, when using Adam optimizer, CNL is able to successfully inject nearly all (95.6%-100.0%) required knowledge while exhibiting zero forgetting.

Additionally, the dynamic characteristic of learning and forgetting is analyzed in Appendix H. Although CNL freezes conflicting neurons and trains only collaborative neurons, its learning efficiency remains comparable to that of conventional FT. This further demonstrates the engineering potential of our CNL.

5.3 Extending CNL to More Complex Datasets

To further validate CNL on more complex datasets, **MMLU**, **MedQA**, **ARC-C**, and **CSQA** were merged into a unified dataset, referred to as **MMAC**. The performance of FT and CNL on MMAC is studied in Appendix I.

Results demonstrate that, while successfully injecting 95% knowledge into LLMs, FT leads to 91.7% forgetting of mastered knowledge, while CNL exhibits zero forgetting. These findings further demonstrate that CNL can effectively prevent catastrophic forgetting even under more complex and large-scale data conditions.

5.4 Extending CNL to Out-of-Set Generalization

We have verified that CNL achieves zero forgetting under in-set setting. However, it is hard to explicitly obtain all Mastered Set and Injection Set in practice. Therefore, the out-of-set generalization capability of CNL is analyzed.

First, Injection Set \mathcal{I} was split into two disjoint subsets in a 1 : 1 ratio, one used for training and the other reserved for evaluation. The “INJECTION” row of Table 5 demonstrates that CNL still achieves zero forgetting because the loss on Mastered Set can be explicitly calculated.

Subsequently, the same procedure is applied to the Mastered Set \mathcal{M} , as reported in the “MASTERED” row of Table 5. Under this setting, the loss on the evaluation Mastered subset cannot be directly computed and is instead estimated using the training Mastered subset. Due to this estimation error, CNL cannot guarantee a monotonic decrease in the evaluation loss. Nevertheless, while zero forgetting cannot be fully achieved, CNL still substantially alleviates catastrophic forgetting, reducing it by 59.1%–81.7% compared to conventional FT.

Furthermore, the training Mastered subset was combined with Injection Set during training to mitigate forgetting, a strategy known as replay. RP follows the same training setup as FT. Results in the “RP”

Table 5: Performance evaluation under out-of-set setting. *Qwen2.5 1.5B* is selected for experiment. To assess generalization, both Injection Set and Mastered Set were partitioned into training and evaluation subsets. This table reports the learning and forgetting performance on unseen evaluation data, demonstrating the excellent generalization capability of CNL.

METHOD	MMLU		MEDQA		ARC-C		CSQA	
	LEARNED	FORGOT	LEARNED	FORGOT	LEARNED	FORGOT	LEARNED	FORGOT
INJECTION	FT	24 (7.3%)	48 (5.5%)	34 (9.7%)	75 (13.2%)	29 (17.9%)	71 (7.5%)	22 (16.2%)
	CNL	31 (9.5%)	0 (0.0%)	39 (11.1%)	0 (0.0%)	29 (17.9%)	0 (0.0%)	23 (16.9%)
MASTERED	FT	178 (26.3%)	110 (26.0%)	208 (29.5%)	143 (50.4%)	104 (32.1%)	49 (10.4%)	86 (31.6%)
	RP	157 (23.2%)	61 (14.4%)	124 (17.6%)	58 (20.4%)	86 (26.5%)	14 (3.0%)	70 (25.7%)
	CNL	179 (26.4%)	46 (10.9%)	243 (34.5%)	33 (11.6%)	116 (35.8%)	9 (1.9%)	147 (54.0%)

row of Table 5 demonstrate that CNL not only learns more new knowledge but also forgets less mastered knowledge compared to replay.

These results demonstrate that CNL not only achieves zero forgetting under the ideal in-set condition, but also significantly alleviates catastrophic forgetting under more practical out-of-set evaluation settings.

6 Related Work

6.1 Knowledge Injection

Existing knowledge injection methods are broadly categorized into two types: parametric methods and non-parametric methods Doan et al. (2021); Kotha et al. (2023).

Parametric methods directly modify model parameters to encode target knowledge via instruction tuning or continued pre-training, but often suffer from catastrophic forgetting of previously acquired knowledge Singhal et al. (2023); Han et al. (2023); Qiu et al. (2024). Non-parametric methods, such as retrieval-augmented generation, augment model inference with externally retrieved information without directly modifying model parameters Lewis et al. (2020); Ram et al. (2023); Xiong et al. (2024). As a result, they mitigate parameter-level interference, but their effectiveness is constrained by retrieval quality and limited access to implicit knowledge required for complex reasoning Salemi and Zamani (2024); Zhu et al. (2024); Kim et al. (2025) .

6.2 Mitigating Catastrophic Forgetting

Approaches to mitigate catastrophic forgetting have been extensively studied De Lange et al. (2021). Existing strategies generally operate along three dimensions.

Data-based approaches, such as experience replay, mix mastered knowledge with injected knowledge to preserve historical gradient signals, but suffer from storage overhead and privacy concerns. Constraint-based approaches, including PEFT, reduce forgetting by restricting the scope of parameter updates or penalizing large deviations from pretrained weights Wang et al. (2021); Hu et al. (2022). Localization-based approaches, such as knowledge editing methods, attempt to identify and modify task-relevant representation regions to achieve targeted knowledge updates with minimal side effects Meng et al. (2022,2).

Although effective in practice, most existing methods rely on heuristic designs and lack an explicit characterization of when and why forgetting occurs. In contrast, this work seeks to establish a principled connection between forgetting behavior and optimization dynamics.

6.3 Gradient Analysis in Continual Learning

From an optimization perspective, the gradient inner product (or gradient similarity) serves as a fundamental indicator of interference between learning objectives Yu et al. (2020); Liu et al. (2021). When gradients induced by new knowledge conflict with those associated with previously learned knowledge, optimization inevitably degrades prior performance, manifesting as catastrophic forgetting Farajtabar et al. (2020). Previous studies in continual and lifelong learning have leveraged gradient projection or alignment techniques to mitigate such conflicts at a global level Wang et al. (2025).

This work advances this perspective by decomposing gradient inner products at the neuron level, enabling identification of conflicting and collaborative components within the model. By selectively suppressing neuron-level conflicting gradients while preserving collaborative ones, forgetting mitigation is transformed from heuristic data balancing into a theoretically grounded training rule that is compatible with standard optimizers.

Conclusion

Catastrophic forgetting during knowledge injection poses a fundamental challenge to the continual learning capability of LLMs. In this work, we establish a gradient-based theoretical framework to explain the underlying mechanism of catastrophic forgetting. We show that strongly negative gradient similarity is the fundamental cause of forgetting and further leverage this insight to categorize neurons into two types: conflicting neurons, which induce forgetting and account for 50%–75% of all neurons, and collaborative neurons, which mitigate forgetting and account for the remaining 25%–50%.

Based on this analysis, we propose a novel knowledge injection method, CNL, which freezes conflicting neurons and updates only collaborative neurons. We theoretically show that, under the assumption of an infinitesimal learning rate η and exactly known Mastered Set, CNL prevents catastrophic forgetting. Extensive experiments on five LLMs, four datasets, and four optimizers further validate our analysis. CNL achieves zero forgetting under in-set evaluation and reduces catastrophic forgetting by 59.1%–81.7% under more practical out-of-set settings.

Overall, this work provides both theoretical insights and practical solutions for mitigating catastrophic forgetting in knowledge injection, offering a principled foundation for continual knowledge acquisition in LLMs.

Acknowledgments

This work was supported by the Noncommunicable Chronic Diseases-National Science and Technology Major Project under Grants 2024ZD0522702 and 2024ZD0528306, and the National Natural Science Foundation of China under Grant 62433007.

References

- Josh Achiam, Steven Adler, Sandhini Agarwal, Lama Ahmad, Ilge Akkaya, Florencia Leoni Aleman, Diogo Almeida, Janko Altenschmidt, Sam Altman, Shyamal Anadkat, et al. Gpt-4 technical report. *arXiv preprint arXiv:2303.08774*, 2023.
- Xueying Bai, Jinghuan Shang, Yifan Sun, and Niranjan Balasubramanian. Continual learning with global alignment. *Advances in Neural Information Processing Systems*, 37:69976–69998, 2024.
- Peter Clark, Isaac Cowhey, Oren Etzioni, Tushar Khot, Ashish Sabharwal, Carissa Schoenick, and Oyvind Tafjord. Think you have solved question answering? try arc, the ai2 reasoning challenge. *arXiv preprint arXiv:1803.05457*, 2018.
- Matthias De Lange, Rahaf Aljundi, Marc Masana, Sarah Parisot, Xu Jia, Aleš Leonardis, Gregory Slabaugh, and Tinne Tuytelaars. A continual learning survey: Defying forgetting in classification tasks. *IEEE transactions on pattern analysis and machine intelligence*, 44(7):3366–3385, 2021.
- Thang Doan, Mehdi Abbana Bennani, Bogdan Mazoure, Guillaume Rabusseau, and Pierre Alquier. A theoretical analysis of catastrophic forgetting through the ntk overlap matrix. In *International Conference on Artificial Intelligence and Statistics*, pages 1072–1080. PMLR, 2021.

Mehrdad Farajtabar, Navid Azizan, Alex Mott, and Ang Li. Orthogonal gradient descent for continual learning. In *International conference on artificial intelligence and statistics*, pages 3762–3773. PMLR, 2020.

Xiou Ge, Ali Mousavi, Edouard Grave, Armand Joulin, Kun Qian, Benjamin Han, Mostafa Arefiyan, and Yunyao Li. Time sensitive knowledge editing through efficient finetuning. *arXiv preprint arXiv:2406.04496*, 2024.

Aaron Grattafiori, Abhimanyu Dubey, Abhinav Jauhri, Abhinav Pandey, Abhishek Kadian, Ahmad Al-Dahle, Aiesha Letman, Akhil Mathur, Alan Schelten, Alex Vaughan, et al. The llama 3 herd of models. *arXiv preprint arXiv:2407.21783*, 2024.

Tianyu Han, Lisa C Adams, Jens-Michalis Papaioannou, Paul Grundmann, Tom Oberhauser, Alexander Löser, Daniel Truhn, and Keno K Bressem. Medalpaca—an open-source collection of medical conversational ai models and training data. *arXiv preprint arXiv:2304.08247*, 2023.

Dan Hendrycks, Collin Burns, Steven Basart, Andy Zou, Mantas Mazeika, Dawn Song, and Jacob Steinhardt. Measuring massive multitask language understanding. *arXiv preprint arXiv:2009.03300*, 2020.

Edward J Hu, Yelong Shen, Phillip Wallis, Zeyuan Allen-Zhu, Yuanzhi Li, Shean Wang, Lu Wang, and Weizhu Chen. Lora: Low-rank adaptation of large language models. *ICLR*, 1(2), 2022.

Jianheng Huang, Leyang Cui, Ante Wang, Chengyi Yang, Xinting Liao, Linfeng Song, Junfeng Yao, and Jinsong Su. Mitigating catastrophic forgetting in large language models with self-synthesized rehearsals. In Lun-Wei Ku, Andre Martins, and Vivek Srikumar, editors, *Proceedings of the 62nd Annual Meeting of the Association for Computational Linguistics (Volume 1: Long Papers)*, August 2024.

Di Jin, Eileen Pan, Nassim Oufattolle, Wei-Hung Weng, Hanyi Fang, and Peter Szolovits. What disease does this patient have? a large-scale open domain question answering dataset from medical exams. *Applied Sciences*, 11(14):6421, 2021.

Zixuan Ke, Yijia Shao, Haowei Lin, Tatsuya Konishi, Gyuhak Kim, and Bing Liu. Continual pre-training of language models. *arXiv preprint arXiv:2302.03241*, 2023.

Junho Kim, Soyeon Bak, Mingyu Lee, Minju Hong, Songha Kim, Tae-Eui Kam, and SangKeun Lee. Connecting the knowledge dots: Retrieval-augmented knowledge connection for commonsense reasoning. In *Proceedings of the 2025 Conference on Empirical Methods in Natural Language Processing*, pages 23582–23601, 2025.

Diederik P Kingma. Adam: A method for stochastic optimization. *arXiv preprint arXiv:1412.6980*, 2014.

Tomasz Korbak, Hady Elsahar, German Kruszewski, and Marc Dymetman. Controlling conditional language models without catastrophic forgetting. In *International Conference on Machine Learning*, pages 11499–11528. PMLR, 2022.

Suhas Kotha, Jacob Mitchell Springer, and Aditi Raghunathan. Understanding catastrophic forgetting in language models via implicit inference. *arXiv preprint arXiv:2309.10105*, 2023.

Patrick Lewis, Ethan Perez, Aleksandra Piktus, Fabio Petroni, Vladimir Karpukhin, Naman Goyal, Heinrich Küttler, Mike Lewis, Wen-tau Yih, Tim Rocktäschel, et al. Retrieval-augmented generation for knowledge-intensive nlp. *Advances in Neural Information Processing Systems*, 33: 9459–9474, 2020.

Hongyu Li, Liang Ding, Meng Fang, and Dacheng Tao. Revisiting catastrophic forgetting in large language model tuning. *arXiv preprint arXiv:2406.04836*, 2024.

Xinlong Li, Weijieying Ren, Wei Qin, Lei Wang, Tianxiang Zhao, and Richang Hong. Analyzing and reducing catastrophic forgetting in parameter efficient tuning. In *ICASSP 2025-2025 IEEE International Conference on Acoustics, Speech and Signal Processing (ICASSP)*, pages 1–5. IEEE, 2025.

Bo Liu, Xingchao Liu, Xiaojie Jin, Peter Stone, and Qiang Liu. Conflict-averse gradient descent for multi-task learning. *Advances in Neural Information Processing Systems*, 34:18878–18890, 2021.

Ilya Loshchilov and Frank Hutter. Decoupled weight decay regularization. In *International Conference on Learning Representations*, 2019. URL <https://openreview.net/forum?id=Bkg6RiCqY7>.

Yun Luo, Zhen Yang, Fandong Meng, Yafu Li, Jie Zhou, and Yue Zhang. An empirical study of catastrophic forgetting in large language models during continual fine-tuning. *IEEE Transactions on Audio, Speech and Language Processing*, 2025.

Kevin Meng, David Bau, Alex Andonian, and Yonatan Belinkov. Locating and editing factual associations in gpt. In *Advances in Neural Information Processing Systems*, volume 35, pages 17359–17372, 2022.

Kevin Meng, Arnab Sen Sharma, Alex Andonian, Yonatan Belinkov, and David Rabinovich. Mass-editing memory in a transformer. In *arXiv preprint arXiv:2210.07229*, 2022.

Eric Mitchell, Charles Lin, Antoine Bosselut, Christopher D Manning, and Chelsea Finn. Memory-based model editing at scale. In *International Conference on Machine Learning*, pages 15817–15831. PMLR, 2022.

Pengcheng Qiu, Chaoyi Wu, Xiaoman Zhang, Weixiong Lin, Yanfeng Wang, and Weidi Xie. Towards building multilingual language model for medicine. *Nature Communications*, 15(1):8384, 2024.

Ori Ram, Yoav Levine, Itay Dalmédigos, Dor Muhlgay, Amnon Shashua, Kevin Leyton-Brown, and Yoav Shoham. In-context retrieval-augmented language models. *Transactions of the Association for Computational Linguistics*, 11:1316–1331, 2023.

David E Rumelhart, Geoffrey E Hinton, and Ronald J Williams. Learning internal representations by error propagation. Technical report, 1985.

Alireza Salemi and Hamed Zamani. Evaluating retrieval quality in retrieval-augmented generation. In *Proceedings of the 47th International ACM SIGIR Conference on Research and Development in Information Retrieval*, pages 2395–2400, 2024.

Karan Singhal, Shekoofeh Azizi, Tao Tu, S Sara Mahdavi, Jason Wei, Hyung Won Chung, Nathan Scales, Ajay Tanwani, Heather Cole-Lewis, Stephen Pfahl, et al. Large language models encode clinical knowledge. *Nature*, 620:172–180, 2023.

Alon Talmor, Jonathan Herzig, Nicholas Lourie, and Jonathan Berant. Commonsenseqa: A question answering challenge targeting commonsense knowledge. In *Proceedings of the 2019 Conference of the North American Chapter of the Association for Computational Linguistics: Human Language Technologies, Volume 1 (Long and Short Papers)*, pages 4149–4158, 2019.

Xingyu Tan, Xiaoyang Wang, Qing Liu, Xiwei Xu, Xin Yuan, and Wenjie Zhang. Paths-over-graph: Knowledge graph empowered large language model reasoning. In *Proceedings of the ACM on Web Conference 2025*, pages 3505–3522, 2025.

Hugo Touvron, Thibaut Lavril, Gautier Izacard, Xavier Martinet, Marie-Anne Lachaux, Timothée Lacroix, Baptiste Rozière, Naman Goyal, Eric Hambro, Faisal Azhar, et al. Llama: Open and efficient foundation language models. *arXiv preprint arXiv:2302.13971*, 2023.

Chenxu Wang, Yilin Lyu, Zicheng Sun, and Liping Jing. Continual gradient low-rank projection fine-tuning for llms. *arXiv preprint arXiv:2507.02503*, 2025.

Ruize Wang, Duyu Tang, Nan Duan, Zhongyu Wei, Xuan-Jing Huang, Jianshu Ji, Guihong Cao, Daxin Jiang, and Ming Zhou. K-adapter: Infusing knowledge into pre-trained models with adapters. In *Findings of the Association for Computational Linguistics: ACL-IJCNLP 2021*, pages 1405–1418, 2021.

Song Wang, Yaochen Zhu, Haochen Liu, Zaiyi Zheng, Chen Chen, and Jundong Li. Knowledge editing for large language models: A survey. *ACM Computing Surveys*, 57(3):1–37, 2024.

Yichen Wu, Hong Wang, Peilin Zhao, Yefeng Zheng, Ying Wei, and Long-Kai Huang. Mitigating catastrophic forgetting in online continual learning by modeling previous task interrelations via pareto optimization. In *Forty-first international conference on machine learning*, 2024.

Guangzhi Xiong, Qiao Jin, Zhiyong Lu, and Aidong Zhang. Benchmarking retrieval-augmented generation for medicine. In *Findings of the Association for Computational Linguistics: ACL 2024*, pages 6233–6251, 2024.

An Yang, Baosong Yang, Binyuan Hui, Bo Zheng, Bowen Yu, Chang Zhou, Chengpeng Li, Chengyuan Li, Dayiheng Liu, Fei Huang, et al. Qwen2 technical report. *arXiv preprint arXiv:2407.10671*, 2024.

Tianhe Yu, Saurabh Kumar, Abhishek Gupta, Sergey Levine, Karol Hausman, and Chelsea Finn. Gradient surgery for multi-task learning. *Advances in neural information processing systems*, 33: 5824–5836, 2020.

Da-Wei Zhou, Hai-Long Sun, Jingyi Ning, Han-Jia Ye, and De-Chuan Zhan. Continual learning with pre-trained models: A survey. *arXiv preprint arXiv:2401.16386*, 2024.

Yuxuan Zhou, Xien Liu, Xiao Zhang, Chen Ning, Shijin Wang, Guoping Hu, and Ji Wu. Investigating and mitigating catastrophic forgetting in medical knowledge injection through internal knowledge augmentation learning. In *The Thirty-ninth Annual Conference on Neural Information Processing Systems*, 2025.

Kun Zhu, Xiaocheng Feng, Xiyuan Du, Yuxuan Gu, Weijiang Yu, Haotian Wang, Qianglong Chen, Zheng Chu, Jingchang Chen, and Bing Qin. An information bottleneck perspective for effective noise filtering on retrieval-augmented generation. *arXiv preprint arXiv:2406.01549*, 2024.

Xiangrong Zhu, Yuexiang Xie, Yi Liu, Yaliang Li, and Wei Hu. Knowledge graph-guided retrieval augmented generation. *arXiv preprint arXiv:2502.06864*, 2025.

A Dataset Details

To verify our conclusions, we selected four datasets for experimentation: MMLU, MedQA, ARC-C, and CSQA. The data processing method is described as follows:

- **MMLU**: 1/10 subsampling is performed to result in 1, 555 remaining questions.
- **MedQA**: 1/10 subsampling is performed to result in 1, 273 remaining questions.
- **ARC-C**: 1/2 subsampling is performed to result in 1, 270 remaining questions.
- **CSQA**: 1/10 subsampling is performed to result in 1, 096 remaining questions.

B Model Inference Details

Model inference was conducted in a Python (3.12.2) environment, with the main packages including `transformers` (4.48.0) and `torch` (2.2.0). To ensure experimental reproducibility, the temperature was set to 0. Model inference precision was set to FP32, and experiments were conducted on a single A800 GPU.

C Model Inference Results

To identify Mastered Set \mathcal{M} and Injection Set \mathcal{I} , LLMs were asked to answer the questions in the datasets. Correctly answered questions were assigned to Mastered Set \mathcal{M} , while incorrectly answered questions were assigned to Injection Set \mathcal{I} . The distribution of different sets are described in Table. 6.

Table 6: Number of questions in Mastered Set \mathcal{M} and Injection Set \mathcal{I} . “Injection” denotes the number of samples in Injection Set (answered incorrectly), while “Mastered” denotes the number of samples in Mastered Set (answered correctly).

MODEL	MMLU		MEDQA		ARC-C		CSQA	
	INJECTION	MASTERED	INJECTION	MASTERED	INJECTION	MASTERED	INJECTION	MASTERED
<i>Qwen 1.5B</i>	678	877	704	568	324	946	272	824
<i>Qwen 3B</i>	585	970	639	633	212	1058	243	853
<i>Qwen 7B</i>	454	1101	502	770	134	1136	197	899
<i>LLAMA 1B</i>	1126	429	952	320	954	316	697	399
<i>LLAMA 3B</i>	727	828	508	764	347	923	308	788

D Model Training Details

The environment of model training was essentially the same as that for model inference. The number of epochs was set to 25. For the SGD optimizer, the learning rate included three values according to their magnitude of gradient: 2e-9, 2e-7, and 1e-7 (see the code for exact configurations). For Momentum optimizer, the learning rate was consistent with SGD, and the momentum coefficient was set to 0.9. For Adam optimizer (without regularization), β_1 and β_2 were 0.9 and 0.999 respectively, and ϵ was 1e-8. For AdamW optimizer, the regularization parameter (weight decay) was 1e-1. Model training was performed in FP32 precision on a single NVIDIA A800 GPU.

E Model Training Results

The samples in Injection Set \mathcal{I} were trained for knowledge injection. After training, the number of correctly answered questions in Injection Set \mathcal{I} was employed to evaluate learning, while the number of incorrectly answered questions in Mastered Set \mathcal{M} was employed to evaluate forgetting. The results in Table. 7 indicates that serious catastrophic forgetting happens during knowledge injection.

F Evaluation on Parameter-Efficient Fine-Tuning

We evaluate LoRA as a representative parameter-efficient fine-tuning (PEFT) baseline.

Table 7: Learning and forgetting during knowledge injection. Results are presented in the format of “Number of Items (Percentage)”. After training, although new knowledge is successfully injected into LLMs, severe catastrophic forgetting is also observed.

MODEL	MMLU		MEDQA		ARC-C		CSQA	
	LEARNED	FORGOT	LEARNED	FORGOT	LEARNED	FORGOT	LEARNED	FORGOT
<i>Qwen 1.5B</i>	168 (24.8%)	188 (21.4%)	191 (27.1%)	264 (46.5%)	104 (32.1%)	88 (9.3%)	86 (31.6%)	163 (19.8%)
<i>Qwen 3B</i>	114 (19.5%)	126 (13.0%)	119 (18.6%)	160 (25.3%)	71 (33.5%)	286 (27.0%)	77 (31.7%)	105 (12.3%)
<i>Qwen 7B</i>	127 (28.0%)	193 (17.5%)	110 (21.9%)	169 (21.9%)	62 (46.3%)	19 (1.7%)	68 (34.5%)	48 (5.3%)
<i>LLaMA 1B</i>	158 (14.0%)	73 (17.0%)	105 (11.0%)	43 (13.4%)	328 (34.4%)	154 (48.7%)	333 (47.8%)	176 (44.1%)
<i>LLaMA 3B</i>	133 (18.3%)	96 (11.6%)	113 (22.2%)	101 (13.2%)	85 (24.5%)	76 (8.2%)	60 (19.5%)	35 (4.4%)

All experiments are conducted on the Qwen2.5-1.5B model. For a fair comparison with standard fine-tuning (Appendix D), we adopt the same training protocol, using the SGD optimizer with a learning rate of $\eta = 1 \times 10^{-5}$. The LoRA configuration employs a rank of $r = 16$ and a scaling factor of $\alpha = 32$, with LoRA modules applied to all linear layers in the attention mechanism. The batch size and number of training epochs are identical to those used in Appendix D.

As shown in Table 8, LoRA achieves learning performance comparable to full fine-tuning, but does not alleviate catastrophic forgetting, exhibiting similarly severe forgetting across all evaluated datasets.

Table 8: Comparison of FT and LoRA under during knowledge injection. Forgetting cannot be effectively prevented when LoRA is employed.

METHOD	MMLU		MEDQA		ARC-C		CSQA	
	LEARNED	FORGOT	LEARNED	FORGOT	LEARNED	FORGOT	LEARNED	FORGOT
FT	168 (24.8%)	188 (21.4%)	191 (27.1%)	264 (46.5%)	104 (32.1%)	88 (9.3%)	86 (31.6%)	163 (19.8%)
LORA	168 (24.8%)	176 (20.1%)	193 (27.4%)	286 (50.4%)	104 (32.1%)	79 (8.4%)	86 (31.6%)	164 (19.9%)

G Theoretical Derivation for More Complex Optimizers

G.1 Momentum Optimizer

When performing gradient descent with learning rate η , the update rule for parameters θ in the Momentum optimizer is as follows:

$$\begin{aligned} m &\leftarrow \beta m + \nabla_{\theta} \mathcal{L}^{\mathcal{I}}(\theta) \\ \theta &\leftarrow \theta - \eta m \end{aligned} \tag{22}$$

where m performs an exponential weighted average of historical gradients for accelerated convergence. $\beta \in [0, 1]$ is the momentum coefficient, used to control the decay rate of historical momentum information.

The impact of parameter updates on existing knowledge is analyzed. Similar to Eq. (9), we perform a Taylor expansion on loss function $\mathcal{L}^{\mathcal{M}}(\theta)$ over Mastered Set

$$\begin{aligned} \mathcal{L}^{\mathcal{M}}(\theta) &= \mathcal{L}^{\mathcal{M}}(\theta - \eta m) \\ &\approx \mathcal{L}^{\mathcal{M}}(\theta) + \nabla_{\theta} \mathcal{L}^{\mathcal{M}}(\theta)^{\top} (-\eta m) \end{aligned} \tag{23}$$

The change in loss on Mastered Set is:

$$\Delta \mathcal{L}^{\mathcal{M}} \approx -\eta \underbrace{\nabla_{\theta} \mathcal{L}^{\mathcal{M}}(\theta)^{\top} m}_{S^{mom}(\mathcal{M}, \mathcal{I})} \quad (24)$$

Here, $S^{mom}(\mathcal{M}, \mathcal{I})$ is defined as the momentum similarity. If $S^{mom} < 0$, then $\Delta \mathcal{L}^{\mathcal{M}} > 0$, leading to forgetting. Utilizing the additivity of inner product, we decompose the global momentum similarity onto each neuron

$$S^{mom}(\mathcal{M}, \mathcal{I}) = \sum_{j=1}^{|\theta|} s_{\theta_j}^{mom} \quad (25)$$

where $s_{\theta_j}^{mom} = \nabla_{\theta_j} \mathcal{L}^{\mathcal{M}}(\theta) \cdot m_j$. Based on the sign of $s_{\theta_j}^{mom}$, we classify the neurons into two categories:

$$\begin{aligned} \theta_{CF} &:= \left\{ \theta_j \mid s_{\theta_j}^{mom}(\mathcal{M}, \mathcal{I}) < 0 \right\} \quad (\text{Conflicting Neurons}) \\ \theta_{CO} &:= \left\{ \theta_j \mid s_{\theta_j}^{mom}(\mathcal{M}, \mathcal{I}) \geq 0 \right\} \quad (\text{Collaborative Neurons}) \end{aligned} \quad (26)$$

Similar to CNL with SGD, the parameter update rule of CNL for momentum is

$$\theta \leftarrow \theta - \eta [\mathbb{I}(S^{mom} \geq 0) \odot m] \quad (27)$$

Under this rule, the loss in Master Set is

$$\begin{aligned} \Delta \mathcal{L}^{\mathcal{M}} &\approx -\eta \nabla_{\theta} \mathcal{L}^{\mathcal{M}}(\theta)^{\top} [\mathbb{I}(S^{mom} \geq 0) \odot m] \\ &= -\eta \sum_{j=1}^{|\theta|} \left[I(s_{\theta_j}^{mom} \geq 0) \cdot (\nabla_{\theta_j} \mathcal{L}^{\mathcal{M}}(\theta) \cdot m_j) \right] \\ &= -\eta \sum_{j=1}^{|\theta|} \left[I(s_{\theta_j}^{mom} \geq 0) \cdot s_{\theta_j}^{mom} \right] \leq 0 \end{aligned} \quad (28)$$

In practical settings, it is nearly impossible for all gradients to be exactly zero. Therefore we get

$$\Delta \mathcal{L}^{\mathcal{M}} < 0 \quad (29)$$

G.2 Adam Optimizer (without weight decay)

The conventional update rule for the Adam optimizer is as follows:

$$\begin{aligned} m &\leftarrow \beta_1 m + (1 - \beta_1) g_t \\ v &\leftarrow \beta_2 v + (1 - \beta_2) g_t^2 \\ \hat{m} &= \frac{m}{1 - \beta_1^t}, \quad \hat{v} = \frac{v}{1 - \beta_2^t} \quad (\text{bias correction}) \\ \theta &\leftarrow \theta - \eta \frac{\hat{m}}{\sqrt{\hat{v}} + \epsilon} \end{aligned} \quad (30)$$

where $g_t = \nabla_{\theta} \mathcal{L}^{\mathcal{I}}(\theta)$ represents the gradient vector at step t . m and v are the exponential moving average estimates of the first moment (mean) and the second raw moment (uncentered variance) of the gradients, respectively. $\beta_1, \beta_2 \in [0, 1]$ are the exponential decay rates for the first and second moment estimates, respectively. \hat{m} and \hat{v} are the bias-corrected moment estimates, intended to counteract the bias caused by initializing m, v to zero during the initial training phase. ϵ is a numerical stability constant added to prevent division by zero.

For notational convenience, we denote the actual update direction calculated by Adam as the vector U_{adam}

$$U^{adam} = \frac{\hat{m}}{\sqrt{\hat{v}} + \epsilon} \quad (31)$$

Therefore, the conventional update rule for the Adam optimizer is

$$\theta = \theta - \eta U^{adam}. \quad (32)$$

Next, we analyze the impact of parameter updates on existing knowledge. We perform a Taylor expansion on the loss function $\mathcal{L}^{\mathcal{M}}(\theta)$ over the mastered set:

$$\begin{aligned}\mathcal{L}^{\mathcal{M}}(\theta) &= \mathcal{L}^{\mathcal{M}}(\theta - \eta U^{adam}) \\ &\approx \mathcal{L}^{\mathcal{M}}(\theta) + \nabla_{\theta} \mathcal{L}^{\mathcal{M}}(\theta)^{\top} (-\eta U^{adam})\end{aligned}\tag{33}$$

The change in loss on the mastered set is:

$$\Delta \mathcal{L}^{\mathcal{M}} \approx -\eta \underbrace{\nabla_{\theta} \mathcal{L}^{\mathcal{M}}(\theta)^{\top} U^{adam}}_{S^{adam}(\mathcal{M}, \mathcal{I})}\tag{34}$$

Here, $S^{adam}(\mathcal{M}, \mathcal{I})$ is defined as the Adam similarity. If $S^{adam} < 0$, then $\Delta \mathcal{L}^{\mathcal{M}} > 0$, leading to forgetting.

Utilizing the additivity of the inner product, we decompose the global Adam similarity onto each neuron:

$$S^{adam}(\mathcal{M}, \mathcal{I}) = \sum_{j=1}^{|\theta|} s_{\theta_j}^{adam}\tag{35}$$

where the similarity component of the j -th neuron is:

$$s_{\theta_j}^{adam} = \nabla_{\theta_j} \mathcal{L}^{\mathcal{M}}(\theta) \cdot U_j^{adam}\tag{36}$$

We classify the neurons into two categories:

$$\begin{aligned}\theta_{CF} &:= \{\theta_j \mid s_{\theta_j}^{adam} < 0\} \quad (\text{Conflicting Neurons}) \\ \theta_{CO} &:= \{\theta_j \mid s_{\theta_j}^{adam} \geq 0\} \quad (\text{collaborative Neurons})\end{aligned}\tag{37}$$

The modified CNL parameter update formula is:

$$\theta \leftarrow \theta - \eta [\mathbb{I}(S^{adam} \geq 0) \odot U^{adam}]\tag{38}$$

Substituting the CNL update rule back into the Taylor expansion of $\Delta \mathcal{L}^{\mathcal{M}}$:

$$\begin{aligned}\Delta \mathcal{L}^{\mathcal{M}} &\approx -\eta \nabla_{\theta} \mathcal{L}^{\mathcal{M}}(\theta)^{\top} [\mathbb{I}(S^{adam} \geq 0) \odot U^{adam}] \\ &= -\eta \sum_{j=1}^{|\theta|} \left[I(s_{\theta_j}^{adam} \geq 0) \cdot (\nabla_{\theta_j} \mathcal{L}^{\mathcal{M}}(\theta) \cdot U_j^{adam}) \right] \\ &= -\eta \sum_{j=1}^{|\theta|} [I(s_{\theta_j}^{adam} \geq 0) \cdot s_{\theta_j}^{adam}] \leq 0\end{aligned}\tag{39}$$

In practical engineering,

$$\Delta \mathcal{L}^{\mathcal{M}} < 0\tag{40}$$

G.3 AdamW Optimizer

The AdamW optimizer introduces decoupled weight decay on top of Adam, separating the weight decay term from the gradient update. Its update rule is as follows:

$$\begin{aligned}m &\leftarrow \beta_1 m + (1 - \beta_1) g_t \\ v &\leftarrow \beta_2 v + (1 - \beta_2) g_t^2 \\ \hat{m} &= \frac{m}{1 - \beta_1^t}, \quad \hat{v} = \frac{v}{1 - \beta_2^t} \\ \theta &\leftarrow \theta - \eta \left(\frac{\hat{m}}{\sqrt{\hat{v}} + \epsilon} + \lambda \theta \right)\end{aligned}\tag{41}$$

where the definitions of $m, v, \hat{m}, \hat{v}, \beta_1, \beta_2, \epsilon$ are consistent with the Adam optimizer. λ represents the Weight Decay Coefficient. Note that the update vector U_{adamw} here includes not only the gradient-based adaptive step size but also the regularization term $\lambda \theta$ pointing towards the origin.

For notational convenience, we denote the actual total update direction calculated by AdamW (including weight decay) as the vector U^{adamw} :

$$U^{adamw} = \frac{\hat{m}}{\sqrt{\hat{v}} + \epsilon} + \lambda\theta \quad (42)$$

The rule of parameter update becomes

$$\theta = \theta - \eta U^{adamw}. \quad (43)$$

Next, we analyze the impact of parameter updates on existing knowledge. We perform a Taylor expansion on the loss function $\mathcal{L}^{\mathcal{M}}(\theta)$ over the mastered set:

$$\begin{aligned} \mathcal{L}^{\mathcal{M}}(\theta) &= \mathcal{L}^{\mathcal{M}}(\theta - \eta U^{adamw}) \\ &\approx \mathcal{L}^{\mathcal{M}}(\theta) + \nabla_{\theta} \mathcal{L}^{\mathcal{M}}(\theta)^{\top} (-\eta U^{adamw}) \end{aligned} \quad (44)$$

The change in loss on Mastered Set is:

$$\Delta \mathcal{L}^{\mathcal{M}} \approx -\eta \underbrace{\nabla_{\theta} \mathcal{L}^{\mathcal{M}}(\theta)^{\top} U^{adamw}}_{S^{adamw}(\mathcal{M}, \mathcal{I})} \quad (45)$$

Here, $S^{adamw}(\mathcal{M}, \mathcal{I})$ is defined as the AdamW similarity. If $S^{adamw} < 0$, then $\Delta \mathcal{L}^{\mathcal{M}} > 0$, leading to forgetting.

Utilizing the additivity of the inner product, we decompose the global AdamW similarity onto each neuron

$$S^{adamw}(\mathcal{M}, \mathcal{I}) = \sum_{j=1}^{|\theta|} s_{\theta_j}^{adamw} \quad (46)$$

where the similarity component of the j -th neuron is:

$$s_{\theta_j}^{adamw} = \nabla_{\theta_j} \mathcal{L}^{\mathcal{M}}(\theta) \cdot U_j^{adamw} \quad (47)$$

We classify the neurons into two categories:

$$\begin{aligned} \theta_{CF} &:= \{\theta_j \mid s_{\theta_j}^{adamw} < 0\} \quad (\text{Conflicting Neurons}) \\ \theta_{CB} &:= \{\theta_j \mid s_{\theta_j}^{adamw} \geq 0\} \quad (\text{collaborative Neurons}) \end{aligned} \quad (48)$$

The modified CNL parameter update formula is

$$\theta \leftarrow \theta - \eta [I(S^{adamw} \geq 0) \odot U^{adamw}] \quad (49)$$

Substituting the CNL update rule back into the Taylor expansion of $\Delta \mathcal{L}^{\mathcal{M}}$:

$$\begin{aligned} \Delta \mathcal{L}^{\mathcal{M}} &\approx -\eta \nabla_{\theta} \mathcal{L}^{\mathcal{M}}(\theta) \cdot [I(S^{adamw} \geq 0) \odot U^{adamw}] \\ &= -\eta \sum_{j=1}^{|\theta|} [I(s_{\theta_j}^{adamw} \geq 0) \cdot (\nabla_{\theta_j} \mathcal{L}^{\mathcal{M}}(\theta) \cdot U_j^{adamw})] \\ &= -\eta \sum_{j=1}^{|\theta|} [I(s_{\theta_j}^{adamw} \geq 0) \cdot s_{\theta_j}^{adamw}] \leq 0 \end{aligned} \quad (50)$$

In practical engineering

$$\Delta \mathcal{L}^{\mathcal{M}} < 0 \quad (51)$$

G.4 General Optimizers

To derive a unified theoretical framework, we abstract the specific update rules of different optimizers into a generalized form. Regardless of whether the optimizer utilizes momentum, adaptive learning rates, or weight decay, its parameter update can ultimately be expressed as applying a specific update vector $F^{opt}(\nabla_{\theta} \mathcal{L}^{\mathcal{T}}(\theta))$ to the current parameters.

The general update rule is defined as:

$$\theta \leftarrow \theta - \eta F^{opt}(\nabla_{\theta} \mathcal{L}^{\mathcal{I}}(\theta)) \quad (52)$$

where η is the global learning rate. Next, we analyze the impact of this general parameter update on existing knowledge. We perform a Taylor expansion on the loss function $\mathcal{L}^{\mathcal{M}}(\theta)$ over the mastered set

$$\begin{aligned} \mathcal{L}^{\mathcal{M}}(\theta) &= \mathcal{L}^{\mathcal{M}}(\theta - \eta F^{opt}(\nabla_{\theta} \mathcal{L}^{\mathcal{I}}(\theta))) \\ &\approx \mathcal{L}^{\mathcal{M}}(\theta) - \eta \nabla_{\theta} \mathcal{L}^{\mathcal{M}}(\theta)^{\top} F^{opt}(\nabla_{\theta} \mathcal{L}^{\mathcal{I}}(\theta)) \end{aligned} \quad (53)$$

The change in loss on the mastered set is:

$$\Delta \mathcal{L}^{\mathcal{M}} \approx -\eta \underbrace{\nabla_{\theta} \mathcal{L}^{\mathcal{M}}(\theta)^{\top} F^{opt}(\nabla_{\theta} \mathcal{L}^{\mathcal{I}}(\theta))}_{S^{opt}(\mathcal{M}, \mathcal{I})} \quad (54)$$

Utilizing the additivity of the inner product, we decompose the global similarity onto each neuron j :

$$S^{opt}(\mathcal{M}, \mathcal{I}) = \sum_{j=1}^{|\theta|} s_{\theta_j}^{opt} \quad (55)$$

where the similarity component of the j -th neuron is determined by the projection of the optimizer's update scalar:

$$s_{\theta_j}^{opt} = \nabla_{\theta_j} \mathcal{L}^{\mathcal{M}}(\theta) \cdot F_j^{opt}(\nabla_{\theta} \mathcal{L}^{\mathcal{I}}(\theta)) \quad (56)$$

Based on the sign of $s_{\theta_j}^{opt}$, we universally classify the neurons into two categories for any optimizer:

$$\begin{aligned} \theta_{CF} &:= \{\theta_j \mid s_{\theta_j}^{opt} < 0\} \quad (\text{Conflicting Neurons}) \\ \theta_{CB} &:= \{\theta_j \mid s_{\theta_j}^{opt} \geq 0\} \quad (\text{Collaborative Neurons}) \end{aligned} \quad (57)$$

The generalized CNL parameter update formula is:

$$\theta \leftarrow \theta - \eta [\mathbb{I}(S^{opt} \geq 0) \odot F^{opt}(\nabla_{\theta} \mathcal{L}^{\mathcal{I}}(\theta))] \quad (58)$$

Substituting the generalized CNL update rule back into the Taylor expansion of $\Delta \mathcal{L}^{\mathcal{M}}$:

$$\begin{aligned} \Delta \mathcal{L}^{\mathcal{M}} &\approx -\eta \nabla_{\theta} \mathcal{L}^{\mathcal{M}}(\theta)^{\top} [\mathbb{I}(S^{opt} \geq 0) \odot F^{opt}(\nabla_{\theta} \mathcal{L}^{\mathcal{I}}(\theta))] \\ &= -\eta \sum_{j=1}^{|\theta|} \left[I(s_{\theta_j}^{opt} \geq 0) \cdot (\nabla_{\theta_j} \mathcal{L}^{\mathcal{M}}(\theta) \cdot F_j^{opt}(\nabla_{\theta} \mathcal{L}^{\mathcal{I}}(\theta))) \right] \\ &= -\eta \sum_{j=1}^{|\theta|} \left[I(s_{\theta_j}^{opt} \geq 0) \cdot s_{\theta_j}^{opt} \right] \leq 0 \end{aligned} \quad (59)$$

In practical engineering, we have:

$$\Delta \mathcal{L}^{\mathcal{M}} < 0 \quad (60)$$

H Dynamic Characteristic of CNL

The dynamic characteristics of learning and forgetting during knowledge injection are shown in Fig. 2. Although CNL freezes conflicting neurons, its training efficiency does not significantly lag behind that of conventional FT.

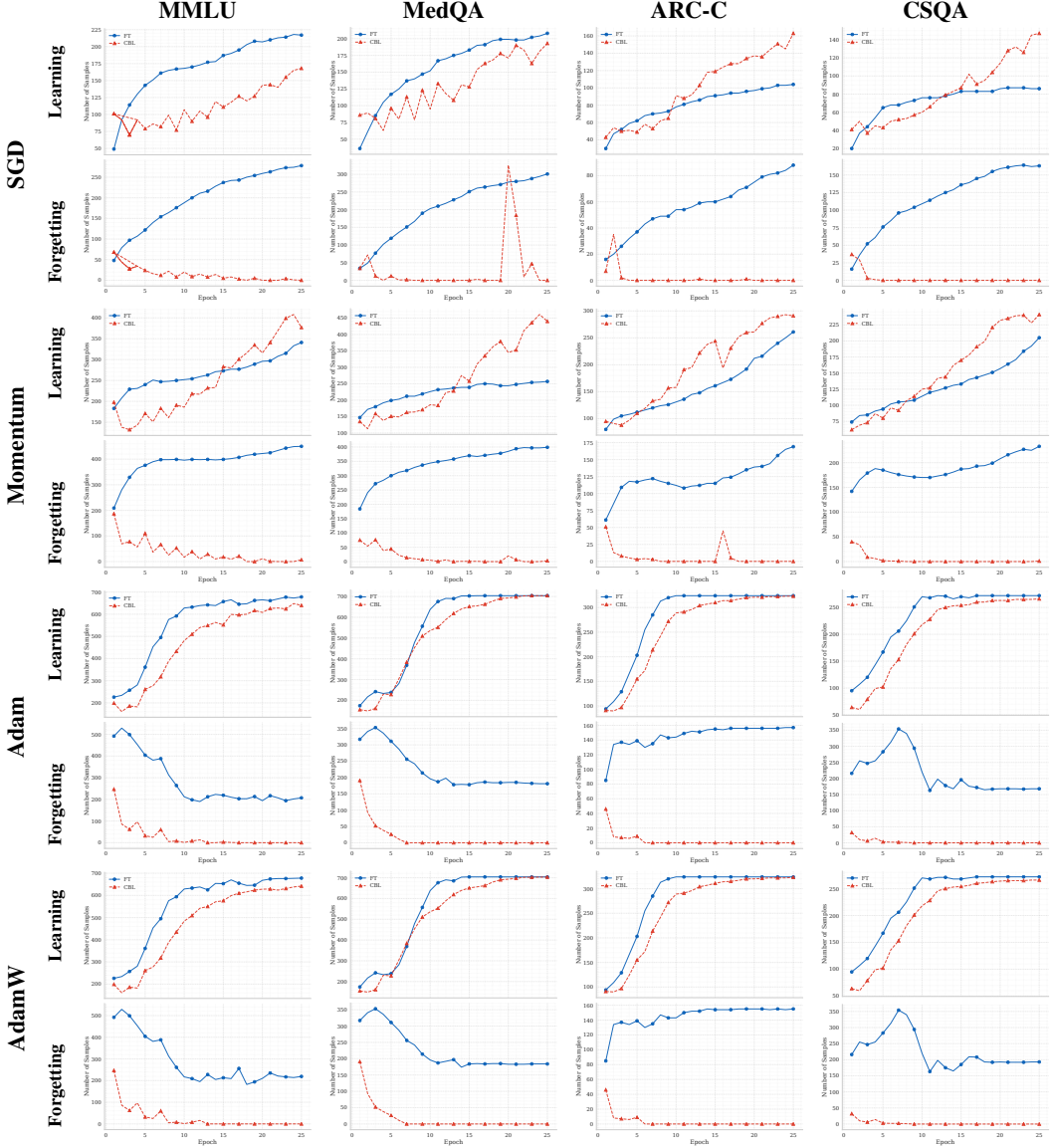


Figure 2: Learning and forgetting curves across four datasets and four optimizers. The rows represent SGD, Momentum, Adam, and AdamW. The inner labels indicate the metric type (Learning vs Forgetting) for the corresponding vertical position.

I Extension to More Complex Dataset

Four datasets, including MMLU, MedQA, ARC-C, and CSQA, were combined to construct a more complex dataset, termed MMAC, to evaluate the performance of CNL on more challenging and diverse data distributions. The performance of learning and forgetting during knowledge injection is summarized in Table 9. Results indicate that FT induced 91.7% forgetting during knowledge injection, while CNL achieves zero forgetting.

Table 9: Performance comparison on MMAC. Even on the larger-scale MMAC dataset, FT causes severe forgetting (91.7%), whereas CNL maintains zero forgetting while achieving high learning accuracy.

METHOD	MMAC		MMLU		MEDQA		ARC-C		CSQA	
	LEARNED	FORGOT	LEARNED	FORGOT	LEARNED	FORGOT	LEARNED	FORGOT	LEARNED	FORGOT
FT	1878 (94.9%)	2949 (91.7%)	625 (92.2%)	806 (91.9%)	665 (94.5%)	547 (96.3%)	316 (97.5%)	819 (86.6%)	272 (100%)	777 (94.3%)
CNL	1893 (95.7%)	0 (0.0%)	604 (89.1%)	0 (0.0%)	700 (99.4%)	0 (0.0%)	321 (99.1%)	0 (0.0%)	268 (98.5%)	0 (0.0%)